HHS Public Access

Author manuscript

Hear Res. Author manuscript; available in PMC 2018 December 01.

Published in final edited form as:

Hear Res. 2017 December ; 356: 25–34. doi:10.1016/j.heares.2017.10.009.

Efferent modulation of pre-neural and neural distortion products

SB Smith[1], **K Ichiba**[1], **DS Velenovsky**[1], and **B Cone**[1]

[1]University of Arizona, Department of Speech, Language, and Hearing Sciences, Tucson, Arizona, USA

Abstract

Distortion product otoacoustic emissions (DPOAEs) and distortion product frequency following responses (DPFFRs) are respectively pre-neural and neural measurements associated with cochlear nonlinearity. Because cochlear nonlinearity is putatively linked to outer hair cell electromotility, DPOAEs and DPFFRs may provide complementary measurements of the human medial olivocochlear (MOC) reflex, which directly modulates outer hair cell function. In this study, we first quantified MOC reflex-induced DPOAE inhibition at spectral fine structure peaks in 22 young human adults with normal hearing. The f1 and f2 tone pairs producing the largest DPOAE fine structure peak for each subject were then used to evoke DPFFRs with and without MOC reflex activation to provide a related *neural* measure of efferent inhibition. We observed significant positive relationships between DPOAE fine structure peak inhibition and inhibition of DPFFR components representing neural phase locking to f2 and 2f1-f2, but not f1. These findings may support previous observations that the MOC reflex inhibits DPOAE sources differentially. That these effects are maintained and represented in the auditory brainstem suggests that the MOC reflex may exert a potent influence on subsequent subcortical neural representation of sound.

Keywords

distortion product otoacoustic emissions; frequency following response; medial olivocochlear reflex; efferent

1. Introduction

The medial olivocochlear (MOC) bundle is an inhibitory neural circuit originating in the mammalian auditory brainstem and terminating directly onto cochlear outer hair cells (OHCs). When activated, the MOC bundle alters OHC motility and indirectly influences basilar membrane motion and inner hair cell (IHC) sensitivity – an effect termed the MOC reflex (Mountain, 1980; Siegel & Kim, 1982; Murugasu & Russell, 1996; Cooper & Guinan,

Corresponding Author Current Address: Spencer B. Smith, Northwestern University, Department of Communication Sciences, 2240 Campus Drive, Evanston, IL 60208, spencer.smith1@northwestern.edu.

Financial disclosures: This research was funded by the National Institutes of Health, National Institute on Deafness and other Communication Disorders (F30 DC01418).

2003, 2006). Experimental work in animal models has demonstrated that although the MOC reflex modulates *pre-neural* signal processing via direct control of the cochlear amplifier, it also influences subsequent *neural* encoding of sound. For example, MOC reflex activation results in "unmasking" of signals-in-noise represented in the auditory nerve (Dolan & Nuttall, 1988; Kawase & Liberman, 1993; Ferry & Meddis, 2007), and this effect appears to be preserved in the behavior of inferior colliculus neurons (Seluakumaran et al., 2008). One proposed function of the MOC reflex based on this data is to peripherally reduce mechano-electrical transduction of noise, which may enhance listening in complex acoustic environments.

The human MOC reflex has been studied almost exclusively using pre-neural assays of OHC function such as otoacoustic emissions (OAEs). OAE-based measurements have revealed characteristics of MOC reflex tuning (e.g., Veuillet et al. 1991; Chéry-Croze et al. 1993; Lilaonitkul and Guinan 2007; Zhao & Dhar, 2012), strength (e.g., Backus & Guinan, 2007; Marshall et al., 2014), and the mechanism's possible involvement in directed auditory attention (e.g., Froehlich et al., 1993; de Boer & Thornton, 2007; Garinis et al., 2011) or listening in noise tasks (e.g., Giraud et al., 1997; Kumar & Vanaja, 2004; de Boer & Thornton, 2008; Smith & Cone, 2015; de Boer et al., 2012). However, a major limitation of this approach is that OAEs are insensitive to MOC reflex effects on the neural ensembles that mediate human hearing, and the functional consequences of this mechanism remain unclear. To directly assess the degree to which efferent-induced changes in inner ear mechanics are maintained beyond the cochlea, it is necessary to understand relationships between pre-neural and neural measurements of the MOC reflex (Lichtenhan et al., 2016; Smith et al., 2017).

1.1. DPOAE Inhibition – A pre-neural MOC reflex assay

Distortion product OAEs (DPOAEs) are sounds putatively generated by cochlear OHCs and recorded in the ear canal. They are evoked by two simultaneously presented pure tones, f1 and f2 with an f2/f1 frequency ratio of 1.22 generating the most robust distortion products (Kemp, 1978; Probst et al., 1991). The 2f1-f2 distortion product is most commonly obtained for clinical and research purposes due to its robustness, although others have been reported in the human literature (e.g., Wittekindt et al., 2009). Distortion products other than 2f1-f2, such as the quadratic distortion product at f2-f1, may prove to be more informative regarding changes in the *in vivo* transducer function; however, these measurements have not been optimized in humans (see Bian & Chen, 2008; Abel et al., 2009).

The contemporary "two source" model of DPOAE generation posits that the ear canal-recorded emission is a mixture of components arising from at least two cochlear initiation sites (Kemp, 1986; Zweig & Shera, 1995; Mauermann et al., 1999 a,b; Shera & Guinan, 1999; Talmadge et al., 1999). The first is the "distortion source" generated by intermodulation distortion of overlapping f1 and f2 traveling waves (Figure 1a), which arises due to the nonlinear growth characteristics of OHC amplification within this region (see Bian et al., 2002, Appendix A). The second is the "reflection source", which arises from coherent scattering of distortion source energy as it reaches its center frequency place on the basilar membrane and travels backward. The recorded DPOAE represents the vector

summation of distortion and reflection source magnitudes and phases as they propagate peripherally from the cochlea and into the ear canal (Kalluri & Shera, 2001). When f1 and f2 are continuously swept or adjusted in small frequency steps, the rate of phase rotation of each source differs significantly and a quasi-periodic "fine structure" of maxima and minima emerges in the DPOAE magnitude-frequency function (Figure 1b) due to constructive and destructive interference of energy from both sources (Brown et al., 1996; Heitmann et al., 1998; Talmadge et al., 1999; Knight & Kemp, 2000, 2001; Dhar & Shaffer, 2004).

Because of the relationship between DPOAEs and OHC motility (Liberman et al., 2002; Cheatham et al., 2004), DPOAEs are sensitive to changes in OHC activity induced by the MOC reflex and provide a non-invasive method to study efferent effects in humans. Most commonly, DPOAEs are recorded first in quiet and then during presentation of a contralateral acoustic stimulus (CAS; e.g., broadband noise), which activates the *uncrossed* fibers of the MOC bundle (Puel & Rebillard, 1990; Chery-Croze et al., 1993; Williams and Brown, 1995, 1997; Guinan, 2006). Amplitude and phase differences between DPOAEs recorded in quiet and with CAS can then be used to quantify attenuation of the cochlear amplifier mediated by the MOC reflex.

An important caveat to consider when measuring DPOAE inhibition is that distortion and reflection sources are differentially affected by CAS (Sun, 2008a; Abdala et al., 2009; Deeter et al., 2009). This occurs because OHCs at distortion and reflection source sites are respectively operating at different "points" on the cochlear amplifier input-output function and the MOC reflex more potently inhibits responses at lower intensities on this function. CAS-induced changes in distortion and reflection source amplitudes and phases can thus combine to cause "artefactual" differences in DPOAE fine structure resulting in gross over- or underestimation of MOC reflex strength (Muller et al., 2005; Wagner et al., 2007; Sun, 2008a; Abdala et al., 2009; Deeter et al., 2009). This issue is minimized and a more accurate estimate of total inhibition is achieved when analyses are conducted at spectral fine structure peaks where reflection and distortion source energy are in phase and constructively interfering. At DPOAE fine structure peaks, average measured inhibition in young, normally hearing adults is ~ 0.5–2.5 dB, depending on frequency and probe tone levels (Lisowska et al., 2002; Zhang et al., 2007; Sun, 2008a; Deeter et al., 2009; Abdala et al., 2009).

1.2. DPFFR Inhibition – A potential *neural* MOC reflex assay

The neural correlates of DPOAEs and their evoking tone pairs can be recorded from electrodes placed on the human scalp (Krishnan, 2007). These "frequency following responses" (FFRs) represent cycle-to-cycle phase locking of auditory nerve and brainstem ensembles to primary tones (F1-FFR and F2-FFR) and multiple distortion product frequencies (Figure 1c). Observations in animals and humans suggest that the 2f1-f2 cubic distortion product FFR (CDP-FFR[1]) is initiated by or tightly coupled to the same nonlinear mechanical cochlear processes that generate the DPOAE reflection source component (Elsisy & Krishnan, 2008). For example, CDP-FFRs may only occur with *monotic* presentation of probe tones with f2/f1 ratios consistent with those used to evoke DPOAEs

[1]We use the notation "CDP-FFR" to refer specifically to the neural 2f1-f2 distortion product. We acknowledge that other cubic (and quadratic) distortion products can sometimes exist in the scalp recorded response.

(Rickman & Chertoff, 1991; Chertoff et al., 1992; Bhagat & Champlin, 2004). Auditory nerve fibers tuned to the 2f1-f2 center frequency place phase-lock at a rate equivalent to the 2f1-f2 period, and the amplitude and phase characteristics of these responses are nearly indistinguishable from those evoked by acoustic pure tones of the same frequency (Goldstein & Kiang, 1968; Kim, 1980; Kim et al., 1980). These findings suggest that the energy evoking CDP-FFRs is present in the gross motion of the 2f1-f2 basilar membrane place, as is the case with the reflection source of the DPOAE. While the distortion source largely contributes to the overall DPOAE amplitude, 2f1-f2 representation in discharge patterns of auditory nerve fibers tuned to the f1 and f2 traveling wave overlap area are relatively weak and obscured by dominant phase locking to the probe tones (Goldstein & Kiang, 1968; Kim et al., 1980). Thus, 2f1-f2 DPOAEs appear to arise from a combination of at least two sources, whereas CDP-FFRs may predominately represent phase locking initiated by the reflection source place (Elsisy & Krishnan, 2008).

F1-FFRs, F2-FFRs, and CDP-FFRs initiated in the auditory nerve are maintained in the phase locking behavior of ventral cochlear nucleus and inferior colliculus neurons (Smoorenburg et al., 1976; Arnold & Burkard, 1998; Faulstich and Kossl, 1999). Given the multiplicity of generators, sources of these scalp-recorded potentials are difficult to disentangle and likely represent overlapping responses from ensembles along the caudo-rostral neuraxis (Stillman et al. 1978; Gardi et al. 1979; Batra et al. 1986; Galbraith et al. 2000, 2001; Bidelman 2015; Shaheen et al., 2015; Tichko & Skoe, 2017). Group delay and latency data suggest that stimulus frequency can be manipulated to bias FFR generators: the rostral brainstem dominates FFR responses to frequencies below ~500 Hz, above which more caudal sources contribute (Batra et al., 1986; King et al., 2016). Beyond ~1000–1500 Hz, neural phase locking becomes poor and pre-neural potentials such as the cochlear microphonic and summating potential can dominate the response. The relationship between stimulus frequency and the dominant neural generator of the scalp recorded response poses important technical considerations in studies comparing DPOAEs and their FFR correlates: f1 and f2 frequencies must not be so high that robust neural responses cannot be obtained; conversely, they must not be so low that DPOAEs have poor signal to noise ratios (SNRs) and CDP-FFRs are dominated by rostral generators further away from their presumed cochlear mechanical source.

Few studies have directly compared DPOAEs and CDP-FFRs and fewer have done so for the purpose of examining pre-neural and neural effects of the MOC reflex. Elsisy and Krishnan (2008) measured input-output functions of simultaneously recorded DPOAEs and CDP-FFRs evoked by low frequency tone pairs. They reported that average DPOAE growth functions were biphasic, whereas average CDP-FFR growth functions were compressive. The authors speculated that the biphasic DPOAE input-output functions may have been influenced by complex interactions between distortion and reflection source components, whereas the CDP-FFR growth functions represented activity only related to the reflection source place. This issue likely also influenced the results of an experiment by Elsisy and Krishnan (2005), wherein CAS during simultaneous DPOAE and CDP-FFR recordings produced DPOAE *enhancements* in some subjects who also showed CDP-FFR inhibition. Assessing DPOAE inhibition only at fine structure peaks may have provided a more straightforward comparison between the two measurements. In a similar study, Bhagat and

Champlin (2004) reported CDP-FFR inhibition with CAS in subjects who also demonstrated DPOAE inhibition. However, the authors differentially optimized stimulus parameters for each type of recording by using different f2/f1 ratios, probe frequencies, and levels and did not measure inhibition at fine structure peaks, making it difficult to directly assess pre-neural and neural effects of the MOC reflex.

1.3. Objectives

We hypothesized that pre-neural and neural distortion products would each be inhibited with activation of the efferent system and that inhibition magnitudes would be related given the apparent mechanical coupling of both responses. By first measuring CAS-induced DPOAE inhibition at spectral fine structure peaks, we were able to avoid responses influenced by vector summation of out of phase source components and thus more accurately measure pre-neural MOC reflex strength. The f1 and f2 combination producing the largest DPOAE fine structure peak for each subject was then used to evoke FFRs with and without CAS to provide a neural measure of efferent inhibition.

2. Methods

2.1. Subjects

The University of Arizona Human Subjects Protection Program approved the following methods. Thirty-one participants, 18 females and 13 males, were recruited for the study. Participant age ranged from 19 – 27 years (Median = 21.4 years). Screening inclusion criteria for enrollment in the study were: (1) No history of neurologic or otologic disease (2) normal otoscopy with no evidence of outer or middle ear disease or cerumen occlusion (3) bilateral air conduction pure tone sensitivity at 20 dB HL or better from 250–8000 Hz (4) type-A tympanograms, defined as peak pressure between ± 50 daPa and peak-compensated static acoustic admittance between 0.4–1.5 mmhos, and (5) a reproducible middle ear muscle reflex threshold to broadband noise (0–10,000 Hz) ≥ 70 dB SPL. Criterion five is based on the consideration that middle ear muscle activation can attenuate DPOAE amplitudes as well as probe tones and therefore confound cochlear efferent measurements (Sun, 2008b; but also see Zhao & Dhar, 2010). Specifically, middle ear muscle reflex thresholds were defined as the lowest levels of CAS needed to elicit a 0.02 mmhos decrease in an ongoing admittance measurement of a 226 Hz probe tone in the right ear (see Discussion for limitations of this approach).

2.2 DPOAE Fine Structure Measurements

During the first visit, DPOAEs were recorded from the right ears of subjects seated comfortably in a sound booth with an ILO 88 OAE System (Otodynamics, Ltd, Hatfield, UK). Proper probe placement was achieved by ensuring that an 80 dB peSPL click stimulus was within +/− 1 dB of target level and that the ear canal transfer function spectrum was visibly flat. DPOAEs were evoked by pure tone pairs (f1<f2; f2/f1=1.22) each calibrated in situ to a level of 70 dB SPL (i.e., L1– L2 = 0). Relatively intense primary tone levels were chosen for this portion of the experiment to ensure that robust neural responses could be recorded using the same stimuli in the second portion of the experiment. While the optimal L1–L2 is widely considered to be 10 – 15 dB (Gaskill & Brown, 1990; Abdala, 1996),

robust 2f1-f2 DPOAEs are indeed detectable using equivalent f1 and f2 levels (e.g., see Figures 1 and 3 in sHauser & Probst, 1991). Three “microstructure” acquisition ranges (each 193–195 Hz wide) centered at f2= 800, 1000, and 1200 Hz, respectively, were used to obtain DPOAEs with 12.2 Hz spectral resolution and therefore reveal emission fine structure within the restricted frequency range of 708 Hz ≤ f2 ≤ 1294 Hz when the measurements were concatenated[2]. This frequency range is lower than the typical “DP-gram” and generally produces recordings with poorer SNRs relative to higher frequency tone pairs (Probst et al., 1990; Gorga et al., 1997). However, constraining f2 below 1500 Hz ensured that the DPOAE stimulus pair producing the largest fine structure peak could also be used to generate sufficiently robust neural responses in the FFR portion of the study.

The three DPOAE microstructure ranges collectively spanning 708 Hz ≤ f2 ≤ 1294 Hz were obtained in ascending order in four interleaved triads of quiet and with CAS trials. The CAS was a 60 dB SPL flat spectrum broadband noise (0–10,000 Hz) presented continuously throughout the recording to the left ear through an ER-2 insert earphone (Etymotic Research, Elk Grove Village, IL). DPOAEs were monitored online, and each point was averaged for approximately 3–4 seconds. Four to five sweeps were obtained for each microstructure frequency range to ensure that noise floors were minimized. Subject data were only considered for further analysis if three consecutive spectral points were ≥ 6 dB above the average noise floor in at least one of the three measured microstructure frequency ranges. Failure to meet this criterion resulted in the exclusion of the subject’s data from further analysis.

DPOAE microstructure data were saved as ASCII files and analyzed offline in MATLAB (The Mathworks, Inc., Natick, MA, USA). First, the three microstructure frequency ranges were combined and plotted as a continuous fine structure spectrum from 708 Hz ≤ f2 ≤ 1294 Hz for each quiet and with CAS trial. Second, the fine structure spectra were averaged and estimates of error at each point were also calculated. This was done differentially for the trials in quiet and those with CAS. Third, the largest fine structure peaks in the quiet and with CAS average spectra were identified using MATLAB’s *findpeaks* function and labeled on the average spectral plots. If the largest amplitude value was at the upper (f2 = 1294) or lower (f2 = 708) margin of the fine structure plot, the second largest peak was selected. f1, f2, and 2f1-f2 frequencies, fine structure peak amplitudes, and inhibition (i.e., fine structure peak amplitude differences between quiet and with CAS) were used in statistical analyses described below. Note that MOC reflex-induced frequency shifts in fine structure peaks have been reported in the literature (e.g., Abdala et al., 2009); however, these shifts are generally smaller (~5–10 Hz) than the spectral resolution of our recordings and were therefore not assessed.

2.3. FFR Measurements

During the second visit, FFRs were recorded from each subject using the Intelligent Hearing Systems Smart-EP advanced research module (Intelligent Hearing Systems, Miami, FL) with a single-channel electrode montage: hairline (+), C7 vertebra (−), and forehead (⏚).

[2]The ILO system acquires DPOAE microstructure data in 193–195 Hz frequency ranges centered at a user-defined test frequency.

FFR stimuli were selected for each subject based on the f1 and f2 pair producing the largest quiet DPOAE fine structure peak in the previous visit. The stimuli were 92 ms pure tones shaped by a trapezoidal envelope with a rise and fall time of 15 ms and presented at 8.1/sec using condensation and rarefaction polarities on separate runs. Both tones were delivered via separate shielded ER-2 insert earphones coupled to an ER 10-B+ probe microphone assembly and acoustically mixed in the ear canal (Etymotic Research, Elk Grove Village, IL). Prior to each recording, the tones were calibrated in-situ to 70 dB SPL using the probe microphone.

Throughout the FFR recordings, subjects remained awake and relaxed in a reclining chair in an electrically-shielded sound booth and electrode impedances were maintained at ≤ 3 kΩ. The EEG was monitored online and recording was paused during obvious subject movements. Individual sweeps with EEG peaks exceeding +/− 20 μV were rejected online as artifact. Response waveforms to condensation and rarefaction stimulus polarities were separately recorded in interleaved quiet and with CAS trials. Individual response waveforms consisted of 2048 artifact-free sweeps amplified 200,000 times and sampled at 40,000 Hz over a 102.4 ms epoch. Responses were online filtered from 10–5000 Hz and more conservatively filtered from 70–2000 Hz offline. Quiet and with CAS trials were repeated either five or six times over the two-hour testing block and waveforms were saved as ASCII files for offline analysis in MATLAB.

The MATLAB program first sorted waveforms into quiet and with CAS conditions and subtracted paired condensation from rarefaction responses within each condition to derive difference waveforms; this technique reduces envelope following responses at f2-f1 (or “ASSRs”) and accentuates F1-FFR, F2-FFR, and CDP-FFR components (Greenberg et al., 1987; Rickman et al., 1991; Krishnan, 1999; Pandya & Krishnan, 2004). Next, the difference waveforms for quiet and with CAS conditions were respectively averaged, weighted with a Hanning window, and a 4096-point fast Fourier transform (FFT) analysis was performed resulting in a spectral bin width of 9.77 Hz. The spectral peaks corresponding to f1, f2, and 2f1-f2 were automatically identified by the MATLAB routine based on each subject’s stimulus tone pair which was manually entered by the user. Amplitudes were expressed in dB re: 1 nV. F1-FFR, F2-FFR and the CDP-FFR were considered “present” if they were each ≥ 6 dB above the noise floor, which was calculated as the average amplitude of the five frequency bins above and below each component. These FFR component amplitudes for quiet and with CAS conditions were used in statistical analyses described below.

2.4. Evaluation of Equipment Distortion and Electromagnetic Stimulus Artifact

OAE and EEG analyzers can themselves generate nonlinear distortion or artifacts mimicking biological responses and thus contaminate experimental data (Chertoff & Hecox, 1990). We assessed non-biological distortion and stimulus artifact contamination of OAE and EEG equipment in pilot experiments conducted prior to recruiting subjects for this study. Non-biological distortion of the ILO 88 system was assessed by sealing the OAE probe tip into a 2-cc coupler and measuring 2f1-f2 spectral amplitude for each of the 51 frequency pairs in the 708 Hz ≤ f2 ≤ 1294 Hz range presented at 70 dB SPL. The average and maximum amplitudes of 2f1-f2 across all tone pairs presented in the coupler were −10.3 dB (± 2.7) and

−4.25 dB, respectively, indicating that non-biologic equipment distortion was minimal. To assess distortion related to stimulus presentation from the EEG equipment, we selected the highest (f1=1060 Hz; f2=1294 Hz) and lowest (f1=580 Hz; f2=708 Hz) possible tone pair combinations that could be used for the FFR portion of this experiment. The probe assembly was inserted into a 2 cc coupler, each tone pair was presented, and waveforms recorded by the ER-10B+ microphone were saved for offline spectral analysis in a custom MATLAB script. Average and maximum spectral amplitude at 2f1-f2 for the two tone pairs was 5.2 dB (± 2.4) and 9.5 dB, respectively, which was inseparable from the spectral noise floor. Lastly, the possibility of stimulus-related electromagnetic artifact contamination of EEG responses was examined. Using the parameters described in Section 2.3., FFRs were collected from one subject in rarefaction and condensation polarities with the highest and lowest possible tone pair combinations. Responses were recorded with earphone tubes open and clamped, respectively, and saved for offline analysis. With open earphone tubes, all F1-FFR, F2-FFR, and CDP-FFR components were identifiable at ≥ 6 dB above the spectral noise floor except for F2-FFR= 1294 Hz. With clamped tubes, no responses were identifiable above the noise floor, suggesting that the EEG was not contaminated by non-biologic electromagnetic artifact.

2.5. Statistical Analyses

DPOAE, F1-FFR, F2-FFR, and CDP-FFR spectral amplitudes identified at ≥ 6 dB above the noise floor were counted to determine the prevalence of these responses under our experimental conditions. A paired t-test was used to assess the effect of noise (quiet vs. with CAS) on DPOAE spectral fine structure amplitude. F1- and F2-FFRs were analyzed separately from the CDP-FFR component due to differences in how the responses are initiated. For example, F1- and F2-FFRs correspond to pure tones with a known input level, whereas the CDP-FFR is initiated by a distortion product of an unknown quantity of energy on the basilar membrane. A two-factor repeated measures analysis of variance (ANOVA) was used to evaluate the effects of spectral peak (F1-FFR and F2-FFR) and Noise (quiet vs. with CAS) on FFR amplitude. A paired t-test was used to assess the effect of noise (quiet vs. with CAS) on CDP-FFR amplitude.

DPOAE and FFR inhibition were calculated by subtracting response amplitudes with CAS from response amplitudes in quiet. Univariate regression analyses between DPOAE inhibition and each FFR peak inhibition measurement were conducted after identifying and removing outliers. Outliers were identified as any value falling outside of 1.5 times the interquartile range above the upper quartile and below the lower quartile.

3. Results

3.1. DPOAE Fine Structure Peak Prevalence and Effects of CAS

DPOAE spectral fine structures from 22 (12 female) out of 31 recruited subjects (71%) met the 6 dB SNR acceptance criteria. Average DPOAE fine structure amplitudes were 12.44 dB (± 4.0) in quiet and 10.79 dB (± 4.27) with CAS, which was a statistically significant difference ($t_{(21)} = 9.90$, $p < 0.005$). The average noise floors corresponding to quiet (−6.51

dB, ± 2.02) and with CAS (−6.02 dB, ± 2.40) fine structure peaks did not significantly differ (p=0.62).

Figure 2a plots DPOAE fine structures in a single subject for quiet (black) and with CAS (red) conditions. Note that the y-axis of each panel is expressed in linear units to visually accentuate response peaks and differences between quiet and with CAS contours. The largest fine structure peak corresponds to f2 = 1111 Hz, which was inhibited by 1.4 dB with CAS. Figure 3 plots DPOAE fine structure inhibition as a function of f2 for all subjects. In all cases, peaks were inhibited with CAS, although the magnitude of inhibition ranged from 0.5–3.5 dB across subjects.

3.2. FFR Peak Prevalence and Effects of CAS

F1-FFRs were most detectable (100%) followed by F2-FFRs (91%) and CDP-FFRs (77%). Figure 2b plots FFR spectra for a single subject for quiet (black) and with CAS (red) conditions using the probe tone pair associated with the DPOAE fine structure peak in 2a. F1-FFR and CDP-FFR inhibition are 2.77 dB and 8.80 dB, respectively. In contrast, F2-FFR exhibited *enhancement* of 3.43 dB in this participant. This was representative of all subjects, as instances of both inhibition and enhancement were observed in FFR peaks during CAS presentation. Inhibition was most prevalent in CDP-FFRs (94%), followed by F2-FFRs (85%) and F1-FFRs (64%).

Figure 4 plots the average amplitudes of each FFR peak in quiet and with CAS. It can be seen that F1-FFR had the largest amplitudes in quiet (55.16 dB) and with CAS (53.92 dB). Further, the F2-FFR and CDP-FFR components had comparable amplitudes in quiet (45.73 dB and 46.71 dB, respectively); however, CAS had a much larger effect on CDP-FFR amplitudes than F2-FFR amplitudes, with an average of 6.8 dB of inhibition for the CDP-FFR and only 1.42 dB for F2-FFR. A two-factor repeated measures ANOVA was conducted on FFR amplitude to evaluate the effects of spectral peak (F1-FFR vs F2-FFR) and noise (quiet vs with CAS). The results demonstrated a significant main effect of spectral peak, ($F[1,21] = 17.69$, $p < 0.0001$), with F1-FFR amplitudes being larger than those for F2-FFR, and a non-significant effect of noise ($F[1,21] = 0.25$, $p=0.62$) or spectral peak/noise interaction ($F[1,21] = 0.06$, $p=0.81$). As shown in Fig. 4, the CAS had no significant effect on F1-FFR or F2-FFR amplitude. However, the 6.8 dB decrement in CDP-FFR with CAS was statistically significant ($t(19) = 5.95$, $p < 0.005$).

3.2. Relationship Between DPOAE and FFR Inhibition Measures

DPOAE, F1-FFR, F2-FFR, and CDP-FFR inhibition values were calculated by subtracting response amplitudes obtained with CAS from those obtained in quiet. Shapiro-Wilk tests of normality on each measurement revealed that DPOAE inhibition was non-normally distributed, which was corrected using a square-root transformation. Inhibition values for FFR peaks were found to be uncorrelated with each other, thus separate univariate analyses between DPOAE inhibition and each FFR peak inhibition measurement were conducted to test the hypothesis that pre-neural inhibition was predictive of neural inhibition (Figure 5). There was a statistically significant relationship between DPOAE inhibition and F2-FFR

inhibition (R^2 = 0.36, p= 0.006) and between DPOAE inhibition and CDP-FFR inhibition (R^2 = 0.39, p= 0.004).

4. Discussion

The present study is the first published report using *complementary* DPOAE fine structure and FFR measurements to explore the relationship between pre-neural and neural MOC reflex effects. The novel findings of this study were that: 1) CAS differentially inhibited FFR peaks associated with stimulus (F1-FFR and F2-FFR) and distortion product (CDP-FFR) components such that the CDP-FFR was most inhibited, and 2) F2-FFR and CDP-FFR inhibition were significantly related to DPOAE fine structure peak inhibition. Our observation that CAS inhibited DPOAE fine structure peaks by 1.65 dB on average is generally consistent with previous reports (Sun, 2008a; Deeter et al., 2009; Abdala et al., 2009). The average magnitude of CDP-FFR inhibition reported in the present study (6.8 dB) falls within the range of previous reports using wideband noise as CAS (Bhagat & Champlin 2004; Elsisy & Krishnan 2005); however, it is imperative to note that none of these studies are parametrically identical.

4.1. The Relationship Between DPOAE Sources and FFR Spectral Peaks

The observed relationships between pre-neural and neural MOC reflex inhibition may be best understood within the context of the two source model of DPOAE generation. According to the model, backward-propagated energy from two cochlear sources contributes to the response measured in the ear canal (Zweig & Shera, 1995; Talmadge et al., 1999). The distortion source arises near or basal to the f2 place where f1 and f2 traveling waves maximally overlap, whereas the reflection source arises from the 2f1-f2 basilar membrane place (Shera & Guinan, 1999; Shera, 2004). Assessing DPOAE inhibition at fine structure peaks minimizes artifacts related to interactions between DPOAE sources and efferent inhibition and thus represents a more accurate measure of the MOC reflex (Abdala et al., 2009). It is important to note that DPOAE measurements obtained in the present study represented a *composite* inhibition of in-phase distortion and reflection sources combined. More sophisticated DPOAE inhibition measurements in which distortion and reflection sources were “unmixed” and appraised individually have revealed that the distortion source component is larger in amplitude than the reflection source component but that the MOC reflex inhibits the reflection component more potently than the distortion component (e.g., Abdala et al., 2009; Deeter et al., 2009). This pattern likely emerges because the energy present on the basilar membrane at the reflection source is less intense and more influenced by cochlear amplifier changes induced by the MOC reflex.

FFR peaks represent forward-fed neural correlates of the DPOAE stimulus pair (F1-FFR and F2-FFR) and, based on data from experimental animals (e.g., Goldstein & Kiang, 1968; Kim, 1980; Kim et al., 1980), mainly the reflection source (CDP-FFR). In this way, the F2-FFR is physiologically coupled to the same basilar membrane place giving rise to the DPOAE *distortion* source and the CDP-FFR is coupled to the same basilar membrane place giving rise to the DPOAE *reflection* source. Thus, an MOC reflex induced change in one of the DPOAE sources may be expected to coincide with a change in its FFR counterpart.

Because we did not unmix DPOAEs and assess inhibition of each source separately[3], we were only able to indirectly assess this relationship in the present study. The observation that F2-FFRs were less inhibited by CAS than CDP-FFRs is consistent with DPOAE reports demonstrating lesser distortion source than reflection source inhibition. Further, the significant relationships between composite DPOAE inhibition and F2- and CDP-FFRs are suggestive that the measures are coupled and similarly influenced by MOC reflex activation. The lack of relationship between DPOAE inhibition and F1-FFR inhibition may be related to the fact that the f1 basilar membrane place is apical to the distortion source and basal to the reflection source; thus, MOC reflex effects at the f1 place may not be represented in the DPOAE inhibition composite measure.

F2-FFR and CDP-FFR inhibition were both larger than DPOAE inhibition on a dB scale; however, the relationship between 1 dB of DPOAE versus FFR inhibition is not straightforward. To directly compare the functional effects of each type of inhibition, it would be necessary to derive a level series function and quantify MOC reflex inhibition in terms of "effective attenuation" (i.e., the amount of stimulus gain in dB needed to overcome the effects of inhibition; see Puria et al., 1996; Lichtenhan et al., 2016, and Smith et al., 2017). Because one presentation level was used in this study, we cannot calculate effective attenuation from our data.

4.2. Experiment Limitations

While the present data provide promise for understanding the relationships between pre-neural and neural efferent effects in humans, our observations should be interpreted with the following limitations and considerations in mind.

Involvement of the middle ear muscle reflex is always a consideration in MOC reflex experiments, as the stimulus and CAS can activate both mechanisms simultaneously (Guinan, 2010). Participants were screened to ensure that contralateral middle ear muscle reflex thresholds were equal to or above 70 dB SPL for the CAS using conventional admittance measurements. Considering evidence that middle ear muscle reflex thresholds may be overestimated using conventional techniques (Feeney & Keefe, 2001; Sun, 2008b; Zhao & Dhar, 2010), it is possible that the CAS may have induced "subthreshold" middle ear muscle activity. Further, the 70 dB SPL tones used to evoke DPOAEs and DPFFRs may have also triggered middle ear muscle activity ipsilaterally or through binaural summation with the CAS. It should be noted, however, that middle ear muscle activation would be expected to attenuate *DPOAEs* more than *FFR* components, as the former are influenced by both forward and backward transmission through the middle ear. The fact that FFR amplitudes were more inhibited with the largest effect seen at the CDP-FFR suggests that the MOC reflex was the dominant source of inhibition. Nevertheless, the possibility of middle ear muscle involvement cannot be fully ruled out in the present experiment.

It is important to consider that even at the pre-neural cochlear level, MOC effects imparted at the base of OHCs are unlikely to proceed "unfiltered" by the many complex drives which

[3]A limitation of constraining f2 within such a small frequency range is that inverse fast Fourier transformation (IFFT) of DPOAE spectra is highly influenced by "boundary effects" (see Mauermann & Kollmeier, 2004) and sources cannot be clearly separated.

activate IHCs (Guinan, 2012, 2014). While it has been demonstrated that the MOC reflex modulates basilar membrane motion (Cooper & Guinan, 2006), IHCs (and consequently auditory nerve fibers) are driven by motion at the top of the *organ of Corti*, not the basilar membrane. Additionally, the effect of CAS on auditory brainstem nuclei is likely much more complex than those imparted by the cochlear efferent system. For example, MOC axons branch collaterally on both OHCs and cochlear nucleus neurons in cat and rodent models (Brown et al., 1988); this suggests that some neural inhibition, while related to MOC fiber activity, is likely not a direct consequence of OHC modulation. It is important to note, however, that collateral MOC fibers have not been identified in humans (Moore & Osen, 1979).

It is also clear that auditory processing of diotic or binaural stimuli becomes more complex at each ascending step of the auditory brainstem (Moore, 1991). We chose the stimulus frequency range in the present study ($708 \leq f2 \leq 1294$ Hz) such that any possible DPOAE fine structure peak would also evoke FFR responses biased towards more caudal brainstem generators (Batra et al., 1986; King et al., 2016) and thus limit the number of processing steps between pre-neural and neural responses. However, the exact sources of our FFRs could not be estimated using neural group delays. Neural group delay measurements are based on the rate of FFR phase change as a function of fine frequency steps. Regions in which the rate of phase change remains constant are suggestive of a stable generator or ensemble of generators (Kuwada et al., 2002; Bharadwadj et al., 2014; Shaheen et al., 2015). The spacing of F1-FFR, F2-FFR, and CDP-FFR components from each subject in the present study was too large for phase data to be unambiguously unwrapped. Thus, the possibility that more rostral neural generators contributed to our recordings cannot be discounted, especially since we used a single vertical electrode montage which is more sensitive to activity in vertically oriented brainstem dipoles (Bidelman et al., 2015; Galbraith et al., 2001; King et al., 2016). Given the periodic nature of our probe stimuli, it is also possible that our FFRs included contributions from cochlear microphonics, especially at higher frequencies. Our few observations of FFR *enhancement* with CAS at higher probe frequencies are consistent with reports that the cochlear microphonic amplitude grows with MOC reflex activation (e.g., Fex, 1959; Aedo et al., 2015). In pilot work for this experiment, we observed that forward masking obliterated F1-FFR, F2-FFR, and CDP-FFR components in four participants, suggesting a neural origin. The possibility that cochlear microphonics were present for some subjects in this experiment, however, cannot be ruled out.

4.3. Future Applications

Simultaneously recorded OAEs and neural responses provide promise for understanding functional efferent effects (Elsisy & Krishnan, 2005, 2008; Wittekindt et al., 2014; Mertes & Leek, 2016). In future experiments, we plan to simultaneously record DPOAEs and FFRs (e.g., Elsisy & Krishnan, 2005, 2008) using small frequency steps or swept tones to account for DPOAE fine structure and to obtain FFR spectra with sufficient resolution for unambiguous phase delay estimates. Such an approach will clarify FFR sources and thus provide a more complete picture regarding the relationship between pre-neural and neural measurements of cochlear distortion and MOC reflex inhibition. Experiments in laboratory animals are also planned to identify the spatial origin(s) of OAE and FFR distortion product

components, and elucidate the hypothesized relationship between pre-neural and neural distortion. For example, slow injection of cell-specific ototoxic pharmaceuticals into the cochlear apex can be used to sequentially manipulate finely spaced cochlear regions, and the time course of distortion product component ablation can identify the region of origination (Lichtenhan et al., 2016). This technique overcomes limitations associated with passive diffusion of ototoxic agents (e.g., limited treatment of the high-frequency, basal half of the cochlear spiral), which is imperative for studying distortion products in OAEs and FFRs from low-frequency stimuli. If the initiation site of the CDP-FFR is indeed from the cochlear apex, this technique could be used to explore cochlear apical function, which is a current limitation of DPOAEs.

References

Abdala C. Distortion product otoacoustic emission (2 f 1- f 2) amplitude as a function of f 2/f 1 frequency ratio and primary tone level separation in human adults and neonates. The Journal of the Acoustical Society of America. 1996; 100(6):3726–3740. [PubMed: 8969474]

Abdala C, Mishra SK, Williams TL. Considering distortion product otoacoustic emission fine structure in measurements of the medial olivocochlear reflex. The Journal of the Acoustical Society of America. 2009; 125(3):1584–1594. [PubMed: 19275316]

Abel C, Wittekindt A, Kössl M. Contralateral acoustic stimulation modulates low-frequency biasing of DPOAE: efferent influence on cochlear amplifier operating state? Journal of neurophysiology. 2009; 101(5):2362–2371. [PubMed: 19279155]

Aedo C, Tapia E, Pavez E, Elgueda D, Delano PH, Robles L. Stronger efferent suppression of cochlear neural potentials by contralateral acoustic stimulation in awake than in anesthetized chinchilla. Frontiers in systems neuroscience. 2015; 9

Arnold S, Burkard R. The auditory evoked potential difference tone and cubic difference tone measured from the inferior colliculus of the chinchilla. The Journal of the Acoustical Society of America. 1998; 104(3 Pt 1):1565–1573. [PubMed: 9745739]

Backus BC, Guinan JJ Jr. Measurement of the distribution of medial olivocochlear acoustic reflex strengths across normal-hearing individuals via otoacoustic emissions. Journal of the Association for Research in Otolaryngology. 2007; 8(4):484–496. [PubMed: 17932717]

Batra R, Kuwada S, Maher VL. The frequency-following response to continuous tones in humans. Hearing research. 1986; 21(2):167–177. [PubMed: 3700255]

Bhagat SP, Champlin CA. Evaluation of distortion products produced by the human auditory system. Hearing research. 2004; 193(1):51–67. [PubMed: 15219320]

Bharadwaj HM, Verhulst S, Shaheen L, Liberman MC, Shinn-Cunningham BG. Cochlear neuropathy and the coding of supra-threshold sound. Frontiers in systems neuroscience. 2014; 8

Bian L, Chen S. Comparing the optimal signal conditions for recording cubic and quadratic distortion product otoacoustic emissions. The Journal of the Acoustical Society of America. 2008; 124(6): 3739. [PubMed: 19206801]

Bidelman GM. Multichannel recordings of the human brainstem frequency-following response: scalp topography, source generators, and distinctions from the transient ABR. Hearing research. 2015; 323:68–80. [PubMed: 25660195]

Brown MC, Liberman MC, Benson TE, Ryugo DK. Brainstem branches from olivocochlear axons in cats and rodents. Journal of Comparative Neurology. 1988; 278(4):591–603. [PubMed: 3230172]

Brown AM, Harris FP, Beveridge HA. Two sources of acoustic distortion products from the human cochlea. J Acoust Soc Am. 1996; 100:3260–3267. [PubMed: 8914308]

Chabert R, Magnan J, Lallemant JG, Uziel A, Puel JL. Contralateral sound stimulation suppresses the compound action potential from the auditory nerve in humans. Otology & neurotology. 2002; 23(5):784–788. [PubMed: 12218635]

Chambers AR, Hancock KE, Maison SF, Liberman MC, Polley DB. Sound-evoked olivocochlear activation in unanesthetized mice. Journal of the Association for Research in Otolaryngology. 2012; 13(2):209–217. [PubMed: 22160753]

Cheatham MA, Huynh KH, Gao J, Zuo J, Dallos P. Cochlear function in Prestin knockout mice. The Journal of physiology. 2004; 560(3):821–830. [PubMed: 15319415]

Chertoff ME, Hecox KE. Auditory nonlinearities measured with auditory-evoked potentials. The Journal of the Acoustical Society of America. 1990; 87(3):1248–1254. [PubMed: 2324391]

Chertoff ME, Hecox KE, Goldstein R. Auditory distortion products measured with averaged auditory evoked potentials. Journal of Speech, Language, and Hearing research. 1992; 35(1):157–166.

Chery-Croze S, Moulin A, Collet L. Effect of contralateral sound stimulation on the distortion product 2f 1- f 2 in humans: Evidence of a frequency specificity. Hearing research. 1993; 68(1):53–58. [PubMed: 8376215]

Cooper NP, Guinan JJ. Separate mechanical processes underlie fast and slow effects of medial olivocochlear efferent activity. The Journal of physiology. 2003; 548(1):307–312. [PubMed: 12611913]

Cooper NP, Guinan JJ. Efferent-mediated control of basilar membrane motion. The Journal of physiology. 2006; 576(1):49–54. [PubMed: 16901947]

de Boer J, Thornton AR. Effects of subject task on contra- lateral suppression of click evoked otoacoustic emissions. Hear Res. 2007; 233(1–2):117–123. [PubMed: 17910996]

de Boer J, Thornton AR. Neural correlates of perceptual learning in the auditory brainstem: Efferent activity predicts and reflects improvement at a speech-in-noise discrimination task. J Neurosci. 2008; 28(19):4929–4937. [PubMed: 18463246]

de Boer J, Thornton AR, Krumbholz K. What is the role of the medial olivocochlear system in speech-in-noise processing? J Neurophysiol. 2012; 107(5):1301–1312. [PubMed: 22157117]

Deeter R, Abel R, Calandruccio L, Dhar S. Contralateral acoustic stimulation alters the magnitude and phase of distortion product otoacoustic emissions. The Journal of the Acoustical Society of America. 2009; 126(5):2413–2424. [PubMed: 19894823]

Dhar S, Shaffer LA. Effects of a suppressor tone on distortion product otoacoustic emissions fine structure: Why a universal suppressor level is not a practical solution to obtaining single-generator DP-grams. Ear and hearing. 2004; 25(6):573–585. [PubMed: 15604918]

Dolan DF, Nuttall AL. Masked cochlear whole-nerve response intensity functions altered by electrical stimulation of the crossed olivocochlear bundle. The Journal of the Acoustical Society of America. 1988; 83(3):1081–1086. [PubMed: 3356813]

Elsisy HM. Comparative study of the frequency following response-distortion products and distortion product otoacoustic emissions in normal hearing adults. 2005

Elsisy H, Krishnan A. Comparison of the acoustic and neural distortion product at 2f1-f2 in normal-hearing adults. International journal of audiology. 2008; 47(7):431–438. [PubMed: 18574781]

Faulstich M, Kössl M. Neuronal response to cochlear distortion products in the anteroventral cochlear nucleus of the gerbil. The Journal of the Acoustical Society of America. 1999; 105(1):491–502. [PubMed: 9921673]

Ferry RT, Meddis R. A computer model of medial efferent suppression in the mammalian auditory system. The Journal of the Acoustical Society of America. 2007; 122(6):3519–3526. [PubMed: 18247760]

Fex J. Preliminary Report: Augmentation of Cochlear Microphonic by Stimulation of Efferent Firres to the Cochlea. Acta oto-laryngologica. 1959; 50(3–6):540–541. [PubMed: 13822583]

Folsom RC, Owsley RM. N1 action potentials in humans: influence of simultaneous contralateral stimulation. Acta oto-laryngologica. 1987; 103(3–4):262–265.

Froehlich P, Collet L, Morgon A. Transiently evoked otoa- coustic emission amplitudes change with changes of directed attention. Physiol Behav. 1993; 53(4):679–682. [PubMed: 8511172]

Galbraith GC, Threadgill MR, Hemsley J, Salour K, Songdej N, Ton J, Cheung L. Putative measure of peripheral and brainstem frequency-following in humans. Neuroscience letters. 2000; 292(2):123–127. [PubMed: 10998564]

Galbraith GC, Bagasan B, Sulahian J. Brainstem frequency-following response recorded from one vertical and three horizontal electrode derivations. Perceptual and motor skills. 2001; 92(1):99–106. [PubMed: 11322612]

Gardi J, Merzenich M, McKean C. Origins of the scalp-recorded frequency-following response in the cat. Audiology. 1979; 18(5):353–380.

Gaskill SA, Brown AM. The behavior of the acoustic distortion product, 2 f 1- f 2, from the human ear and its relation to auditory sensitivity. The Journal of the Acoustical Society of America. 1990; 88(2):821–839. [PubMed: 2212308]

Giraud AL, Garnier S, Micheyl C, Lina G, Chays A, Chery-Croze S. Auditory efferents involved in speech-in-noise intelligibility. Neuroreport. 1997; 8(7):1779–1783. [PubMed: 9189932]

Goldstein JL, Kiang NY. Neural correlates of the aural combination tone 2f 1-f 2. Proceedings of the IEEE. 1968; 56(6):981–992.

Gorga MP, Neely ST, Ohlrich B, Hoover B, Redner J, Peters J. From laboratory to clinic: A large scale study of distortion product otoacoustic emissions in ears with normal hearing and ears with hearing loss. Ear and hearing. 1997; 18(6):440–455. [PubMed: 9416447]

Greenberg S, Marsh JT, Brown WS, Smith JC. Neural temporal coding of low pitch. I. Human frequency-following responses to complex tones. Hearing Research. 1987; 25(2):91–114. [PubMed: 3558136]

Guinan JJ Jr. Olivocochlear efferents: anatomy, physiology, function, and the measurement of efferent effects in humans. Ear and hearing. 2006; 27(6):589–607. [PubMed: 17086072]

Guinan JJ. How are inner hair cells stimulated? Evidence for multiple mechanical drives. Hearing research. 2012; 292(1):35–50. [PubMed: 22959529]

Guinan JJ Jr. Olivocochlear efferent function: issues regarding methods and the interpretation of results. Frontiers in systems neuroscience. 2014; 8

Hauser R, Probst R. The influence of systematic primary-tone level variation L 2- L 1 on the acoustic distortion product emission 2 f 1- f 2 in normal human ears. The Journal of the Acoustical Society of America. 1991; 89(1):280–286. [PubMed: 2002169]

Heitmann J, Waldmann B, Schnitzler H-U, Plinkert PK, Zenner H-P. Suppression of distortion product otoacoustic emissions DPOAE_ near 2f1- f2 removes DP-gram fine structure-evidence for a secondary generator. J Acoust Soc Am. 1998; 103:1527–1531.

Horn JH, Pratt SR, Durrant JD. Parameters to maximize 2f2-f1 distortion product otoacoustic emission levels. Journal of Speech, Language, and Hearing Research. 2008; 51(6):1620–1629.

Kalluri R, Shera CA. Distortion-product source unmixing: A test of the two-mechanism model for DPOAE generation. The Journal of the Acoustical Society of America. 2001; 109(2):622–637. [PubMed: 11248969]

Kawase T, Liberman MC. Antimasking effects of the olivocochlear reflex. I. Enhancement of compound action potentials to masked tones. Journal of Neurophysiology. 1993; 70(6):2519–2532. [PubMed: 8120596]

Kawase T, Takasaka T. The effect of contralateral noise on masked compound action potential in humans. Hearing research. 1995; 91(1):1–6. [PubMed: 8647711]

Kemp DT. Stimulated acoustic emissions from within the human auditory system. The Journal of the Acoustical Society of America. 1978; 64(5):1386–1391. [PubMed: 744838]

Kemp DT. Otoacoustic emissions, travelling waves and cochlear mechanisms. Hearing research. 1986; 22(1):95–104. [PubMed: 3733548]

Kim DO. Cochlear mechanics: implications of electrophysiological and acoustical observations. Hearing research. 1980; 2(3–4):297–317. [PubMed: 7410234]

Kim DO, Molnar CE, Matthews JW. Cochlear mechanics: nonlinear behavior in two-tone responses as reflected in cochlear-nerve-fiber responses and in ear-canal sound pressure. The Journal of the Acoustical Society of America. 1980; 67(5):1704–1721. [PubMed: 7372925]

King A, Hopkins K, Plack CJ. Differential Group Delay of the Frequency Following Response Measured Vertically and Horizontally. Journal of the Association for Research in Otolaryngology. 2016; 17(2):133–143. [PubMed: 26920344]

Knight RD, Kemp DT. Indications of different distortion product otoacoustic emission mechanisms from a detailed f1, f2 area study. The Journal of the Acoustical Society of America. 2000; 107(1): 457–473. [PubMed: 10641654]

Knight RD, Kemp DT. Wave and place fixed DPOAE maps of the human ear. The Journal of the Acoustical Society of America. 2001; 109(4):1513–1525. [PubMed: 11325123]

Krishnan A. Human frequency-following responses to two-tone approximations of steady-state vowels. Audiology and Neurotology. 1999; 4(2):95–103. [PubMed: 9892760]

Krishnan A. Human frequency following response. Auditory evoked potentials: Basic principles and clinical application. 2007:313–335.

Kumar UA, Vanaja CS. Functioning of olivocochlear bundle and speech perception in noise. Ear and hearing. 2004; 25(2):142–146. [PubMed: 15064659]

Kuwada S, Anderson JS, Batra R, Fitzpatrick DC, Teissier N, D'Angelo WR. Sources of the scalp-recorded amplitude-modulation following response. Journal of the American Academy of Audiology. 2002; 13(4):188–204. [PubMed: 12025895]

Lee HY, Raphael PD, Xia A, Kim J, Grillet N, Applegate BE, … Oghalai JS. Two-Dimensional Cochlear Micromechanics Measured In Vivo Demonstrate Radial Tuning within the Mouse Organ of Corti. The Journal of Neuroscience. 2016; 36(31):8160–8173. [PubMed: 27488636]

Liberman MC, Gao J, He DZ, Wu X, Jia S, Zuo J. Prestin is required for electromotility of the outer hair cell and for the cochlear amplifier. Nature. 2002; 419(6904):300–304. [PubMed: 12239568]

Lichtenhan JT, Wilson US, Hancock KE, Guinan JJ. Medial olivocochlear efferent reflex inhibition of human cochlear nerve responses. Hearing Research. 2016; 333:216–224. [PubMed: 26364824]

Lichtenhan JT, Hartsock J, Dornhoffer JR, Donovan KM, Salt AN. Drug delivery into the cochlear apex: Improved control to sequentially affect finely spaced regions along the entire length of the cochlear spiral. Journal of neuroscience methods. 2016; 273:201–209. [PubMed: 27506463]

Lilaonitkul W, Guinan JJ. Reflex control of the human inner ear: a half-octave offset in medial efferent feedback that is consistent with an efferent role in the control of masking. Journal of neurophysiology. 2009; 101(3):1394–1406. [PubMed: 19118109]

Lonsbury-Martin BL, Whitehead ML, Martin GK. Clinical applications of otoacoustic emissions. Journal of Speech, Language, and Hearing Research. 1991; 34(5):964–981.

Maison S, Micheyl C, Collet L. Influence of focused auditory attention on cochlear activity in humans. Psychophysiology. 2001; 38(01):35–40. [PubMed: 11321619]

Marshall L, Miller JAL, Guinan JJ, Shera CA, Reed CM, Perez ZD, … Boege P. Otoacoustic-emission-based medial-olivocochlear reflex assays for humans. The Journal of the Acoustical Society of America. 2014; 136(5):2697–2713. [PubMed: 25373970]

Mauermann M, Uppenkamp S, van Hengel PW, Kollmeier B. Evidence for the distortion product frequency place as a source of distortion product otoacoustic emission (DPOAE) fine structure in humans. I. Fine structure and higher-order DPOAE as a function of the frequency ratio f2/f1. The Journal of the Acoustical Society of America. 1999; 106(6):3473–3483. [PubMed: 10615687]

Mauermann M, Uppenkamp S, van Hengel PW, Kollmeier B. Evidence for the distortion product frequency place as a source of distortion product otoacoustic emission (DPOAE) fine structure in humans. II. Fine structure for different shapes of cochlear hearing loss. The Journal of the Acoustical Society of America. 1999; 106(6):3484–3491. [PubMed: 10615688]

Mertes IB, Leek MR. Concurrent measures of contralateral suppression of transient-evoked otoacoustic emissions and of auditory steady-state responses a. The Journal of the Acoustical Society of America. 2016; 140(3):2027–2038. [PubMed: 27914370]

Moore JK, Osen KK. The human cochlear nuclei. Exp Brain Res Suppl. 1979; 11:36–44.

Moore DR. Anatomy and physiology of binaural hearing. Audiology. 1991; 30(3):125–134. [PubMed: 1953442]

Mountain DC. Changes in endolymphatic potential and crossed olivocochlear bundle stimulation alter cochlear mechanics. Science. 1980; 210(4465):71–72. [PubMed: 7414321]

Murugasu E, Russell IJ. The effect of efferent stimulation on basilar membrane displacement in the basal turn of the guinea pig cochlea. The Journal of neuroscience. 1996; 16(1):325–332. [PubMed: 8613799]

Müller J, Janssen T, Heppelmann G, Wagner W. Evidence for a bipolar change in distortion product otoacoustic emissions during contralateral acoustic stimulation in humans. The Journal of the Acoustical Society of America. 2005; 118(6):3747–3756. [PubMed: 16419819]

Pandya PK, Krishnan A. Human frequency-following response correlates of the distortion product at 2F1-F2. Journal of the American Academy of Audiology. 2004; 15(3):184–197. [PubMed: 15119460]

Perrot X, Ryvlin P, Isnard J, Guénot M, Catenoix H, Fischer C, … Collet L. Evidence for corticofugal modulation of peripheral auditory activity in humans. Cerebral Cortex. 2006; 16(7):941–948. [PubMed: 16151174]

Probst R, Hauser R. Distortion product otoacoustic emissions in normal and hearing-impaired ears. American journal of otolaryngology. 1990; 11(4):236–243. [PubMed: 2240411]

Puel JL, Rebillard G. Effect of contralateral sound stimulation on the distortion product 2F1- F2: Evidence that the medial efferent system is involved. The Journal of the Acoustical Society of America. 1990; 87(4):1630–1635. [PubMed: 2341667]

Rickman MD, Chertoff ME, Hecox KE. Electrophysiological evidence of nonlinear distortion products to two-tone stimuli. The Journal of the Acoustical Society of America. 1991; 89(6):2818–2826. [PubMed: 1918625]

Seluakumaran K, Mulders WH, Robertson D. Unmasking effects of olivocochlear efferent activation on responses of inferior colliculus neurons. Hearing research. 2008; 243(1):35–46. [PubMed: 18573627]

Shaheen LA, Valero MD, Liberman MC. Towards a diagnosis of cochlear neuropathy with envelope following responses. Journal of the Association for Research in Otolaryngology. 2015; 16(6):727–745. [PubMed: 26323349]

Shera CA, Guinan JJ Jr. Evoked otoacoustic emissions arise by two fundamentally different mechanisms: a taxonomy for mammalian OAEs. The Journal of the Acoustical Society of America. 1999; 105(2):782–798. [PubMed: 9972564]

Shera CA. Mechanisms of mammalian otoacoustic emission and their implications for the clinical utility of otoacoustic emissions. Ear and hearing. 2004; 25(2):86–97. [PubMed: 15064654]

Siegel JH, Kim DO. Efferent neural control of cochlear mechanics? Olivocochlear bundle stimulation affects cochlear biomechanical nonlinearity. Hearing research. 1982; 6(2):171–182. [PubMed: 7061350]

Smith SB, Cone B. The medial olivocochlear reflex in children during active listening. International journal of audiology. 2015; 54(8):518–523. [PubMed: 25735203]

Smith SB, Lichtenhan JT, Cone BK. Contralateral Inhibition of Click-and Chirp-Evoked Human Compound Action Potentials. Frontiers in neuroscience. 2017; 11

Smoorenburg GF, Gibson MM, Kitzes LM, Rose JE, Hind JE. Correlates of combination tones observed in the response of neurons in the anteroventral cochlear nucleus of the cat. The Journal of the Acoustical Society of America. 1976; 59(4):945–962. [PubMed: 1262594]

Stillman RD, Crow G, Moushegian G. Components of the frequency-following potential in man. Electroencephalography and Clinical Neurophysiology. 1978; 44(4):438–446. [PubMed: 76552]

Sun XM. Distortion product otoacoustic emission fine structure is responsible for variability of distortion product otoacoustic emission contralateral suppression. The Journal of the Acoustical Society of America. 2008; 123(6):4310–4320. [PubMed: 18537382]

Sun XM. Contralateral suppression of distortion product otoacoustic emissions and the middle-ear muscle reflex in human ears. Hearing research. 2008; 237(1):66–75. [PubMed: 18258398]

Talmadge CL, Long GR, Tubis A, Dhar S. Experimental confirmation of the two-source interference model for the fine structure of distortion product otoacoustic emissions. The Journal of the Acoustical Society of America. 1999; 105(1):275–292. [PubMed: 9921655]

Tichko P, Skoe E. Frequency-dependent fine structure in the frequency-following response: The byproduct of multiple generators. Hearing research. 2017; 348:1–15. [PubMed: 28137699]

Veuillet E, Collet L, Duclaux R. Effect of contralateral acoustic stimulation on active cochlear micromechanical properties in human subjects: dependence on stimulus variables. Journal of Neurophysiology. 1991; 65(3):724–735. [PubMed: 2051201]

Wagner W, Heppelmann G, Müller J, Janssen T, Zenner HP. Olivocochlear reflex effect on human distortion product otoacoustic emissions is largest at frequencies with distinct fine structure dips. Hearing research. 2007; 223(1):83–92. [PubMed: 17137736]

Williams DM, Brown AM. Contralateral and ipsilateral suppression of the 2f1- f 2 distortion product in human subjects. The Journal of the Acoustical Society of America. 1995; 97(2):1130–1140. [PubMed: 7876435]

Williams DM, Brown AM. The effect of contralateral broad-band noise on acoustic distortion products from the human ear. Hearing research. 1997; 104(1):127–146. [PubMed: 9119756]

Wittekindt A, Gaese BH, Kössl M. Influence of contralateral acoustic stimulation on the quadratic distortion product f2–f1 in humans. Hearing research. 2009; 247(1):27–33. [PubMed: 18951964]

Wittekindt A, Kaiser J, Abel C. Attentional modulation of the inner ear: a combined otoacoustic emission and EEG study. The Journal of Neuroscience. 2014; 34(30):9995–10002. [PubMed: 25057201]

Zhang F, Boettcher FA, Sun XM. Contralateral suppression of distortion product otoacoustic emissions: Effect of the primary frequency in Dpgrams. International journal of audiology. 2007; 46(4):187–195. [PubMed: 17454232]

Zhao W, Dhar S. The effect of contralateral acoustic stimulation on spontaneous otoacoustic emissions. Journal of the Association for Research in Otolaryngology. 2010; 11(1):53–67. [PubMed: 19798532]

Zhao W, Dhar S. Frequency tuning of the contralateral medial olivocochlear reflex in humans. Journal of neurophysiology. 2012; 108(1):25–30. [PubMed: 22457463]

Zweig G, Shera CA. The origin of periodicity in the spectrum of evoked otoacoustic emissions. The Journal of the Acoustical Society of America. 1995; 98(4):2018–2047. [PubMed: 7593924]

- We examined relationships between distortion product otoacoustic emission (DPOAE) and distortion product frequency following response (DPFFR) inhibition with contralateral noise
- Both responses were inhibited with contralateral noise
- DPOAE inhibition was related to inhibition of DPFFR components corresponding to f2 and 2f1-f2 frequencies
- Results provide important information regarding the *neural* consequence of efferent inhibition, which has mainly been studied using *pre-neural* assays.

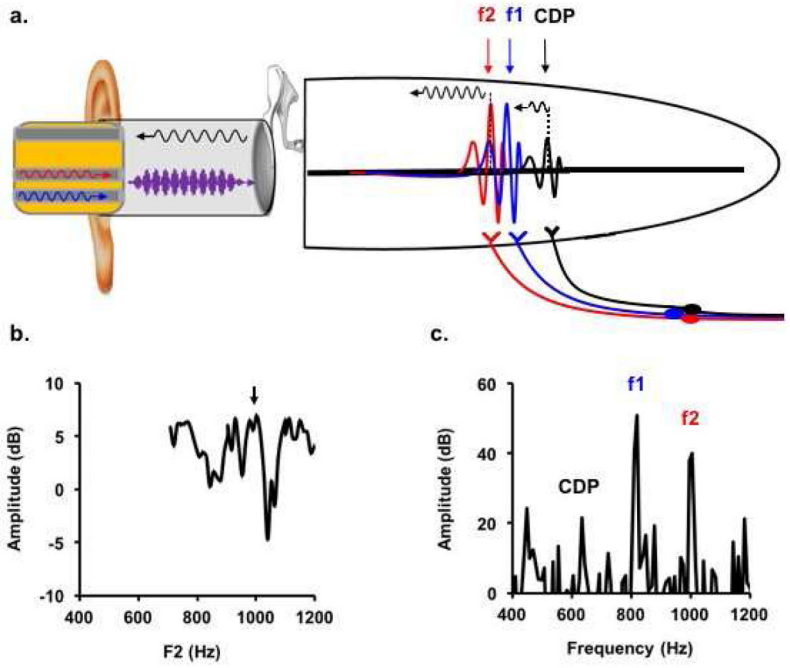

Figure 1.

Pre-neural and neural correlates of the two source model. a) F1 and f2 stimuli (blue and red waveforms, respectively) mix acoustically in the ear canal to form a two-tone complex waveform (purple). The complex waveform is decomposed on the basilar membrane into two cochlear traveling waves representing f1 (blue arrow) and f2 (red arrow) frequencies. Energy from the distortion source, where f1 and f2 traveling waves overlap, propagates backward toward the ear canal and forward to the CDP place. The reflection source arises from coherent scattering of energy at the CDP place, which also propagates toward the ear canal and mixes with distortion source energy. Auditory nerve fibers tuned to f1, f2, and CDP center frequencies feed each component forward into the neural code. b) The DPOAE fine structure represents peaks at which distortion and reflection sources constructively (black arrow) and destructively (subsequent trough) interfere. c) Phase locking to f1, f2, and CDP components initiated by auditory nerve fibers is represented in the ensemble behavior of auditory brainstem nuclei and recorded from the scalp as the FFR. (Note: The f2-f1 (or ASSR) potential corresponding to the amplitude modulated envelope of the two tone stimulus (purple) is not shown.

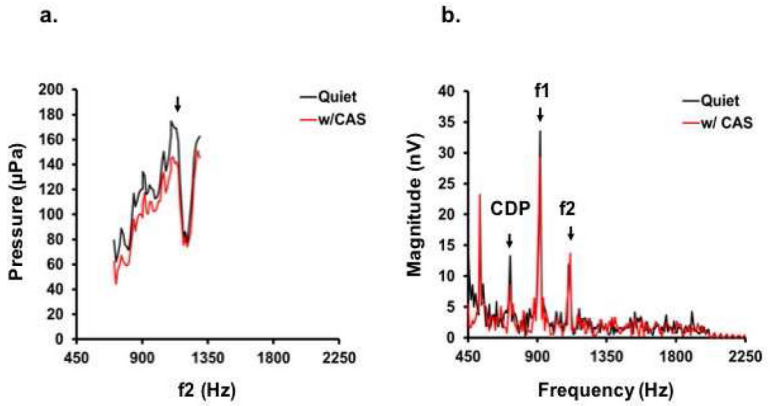

Figure 2.

Effects of CAS on DPOAE fine structure and complementary FFRs in one subject. a) DPOAE fine structure is plotted as a function of f2 on a linear pressure scale. Fine structure is shown in quiet (black) and with CAS (red). The fine structure peak was identified at f2 = 1111 Hz. b) The probe tones corresponding to the DPOAE fine structure peak were used to evoke FFRs. Spectra are plotted for quiet (black line) and with CAS (red line) conditions. *CDP= 721 Hz, F1-FFR = 916 Hz, F2-FFR = 1111 Hz. Note also that an additional FFR corresponding to 3f1-2f2 at 526 Hz is apparent.*

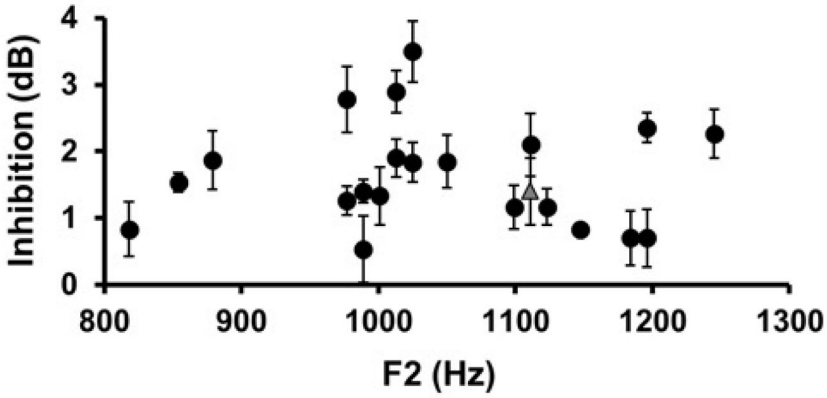

Figure 3.

DPOAE fine structure peak inhibition for each subject plotted as a function of f2 frequency (Error bars = SEM of repeated measurements). The gray triangle corresponds with the subject data shown in Figure 2a.

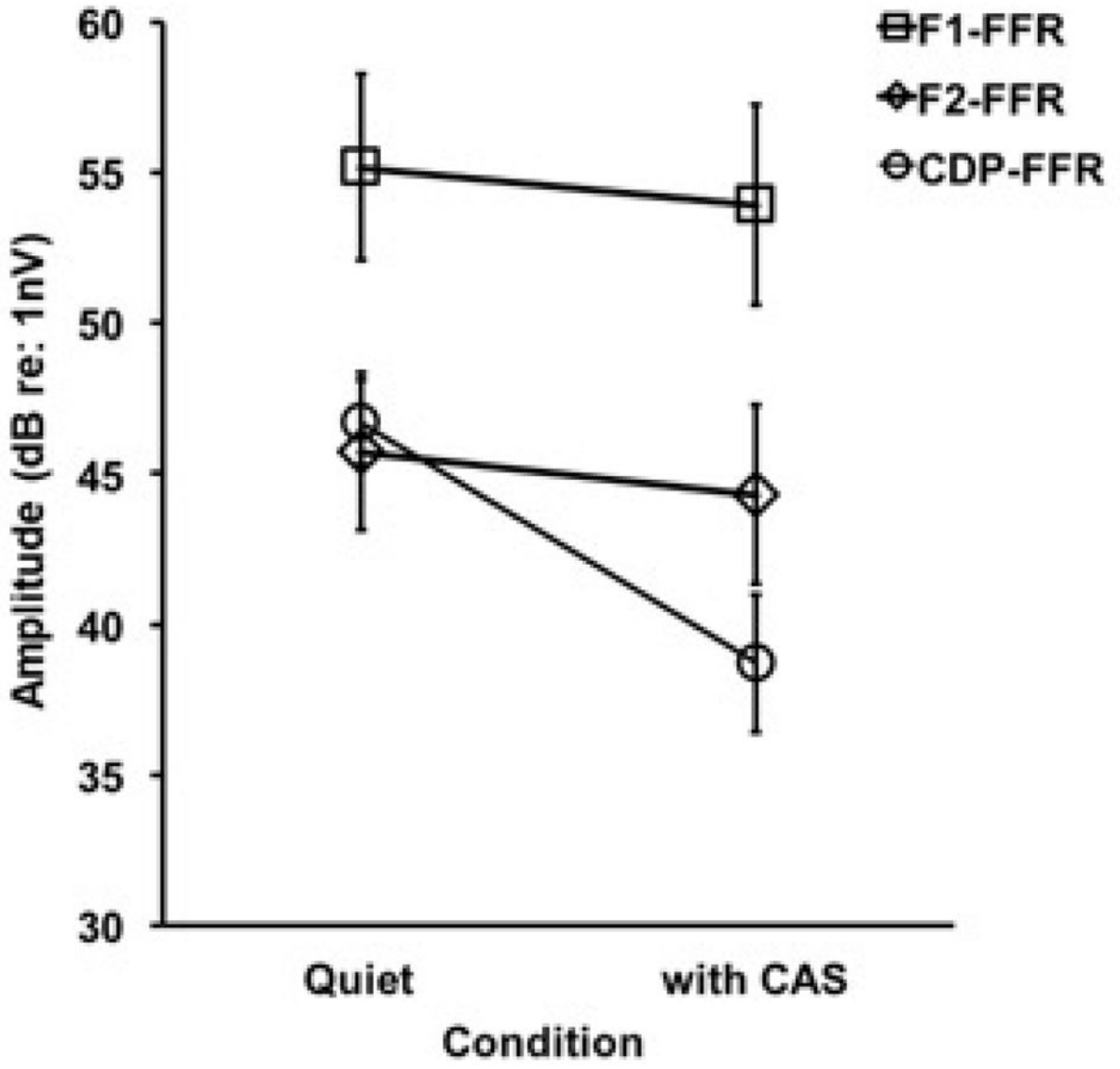

Figure 4.
FFR peak amplitudes in quiet and with CAS (Error Bars = SEM).

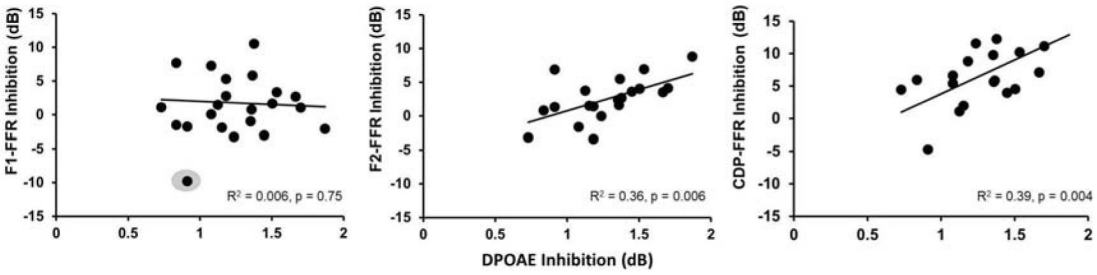

Figure 5.

Scatter plots showing relationships between (square-root transformed) DPOAE inhibition and FFR inhibition as a function of FFR spectral peak. Lines of best fit for each comparison are shown; note that the outlier in the first panel (gray circle) was not included in the model. Regression equations for each comparison were: F1-FFR (y= −0.9473x + 2.95), F2-FFR (y= 5.1641x − 4.252), and CDP-FFR (y = 8.3733x − 3.4955). See text for more detail.